Extended Abstracts of the 2002 International Conference on Solid State Devices and Materials, Nagoya, 2002, pp. 644-645

P11-9

Design and Fabrication of InP/InGaAs HBTs

Kang-Dae Kim, Jae-Hong Park, Yong-Kyu Kim**, Sung-Bum Hwang*** and Chung-Kun Song*
Division of Electrical, Electronics and Computer Eng., Dong-A University
840 Hadan-dong, Saha-gu, Pusan 604-714, Korea
* cksong@daunet.donga.ac.kr , Tel: 051-200-7711, Fax: 051-200-7712
** Department of Mechatronics, Geo Chang Polytechnic College, Kyungnam Geo Chang, 670-800, KOREA
*** Department of Electronics Information Communication
Kyungnam College of Information & Technology, Pusan, 617-701, KOREA

1. Introduction

InP-based HBTs are attractive for high-speed owing to the excellent electron transport property of their materials. The small surface recombination velocities both in InP and InGaAs are also advantages for high-speed/high-density IC's without a serious degradation in the current gain. In this paper, InP-based HBT's have been optimally designed by numerical simulation and fabricated by the self-aligned process. The structure of HBT was designed in terms the current gain*f_{max} for the base and f_T*f_{max} for the collector. The fabricated HBTs produced the current gain of about 50 and the cutoff frequency and the maximum oscillation frequency of 87GHz and 294GHz respectively.

2. Device Design

The material parameters of InP/InGaAs such as energy bandgap, band discontinuities and the electron and hole effective mass parameters are obtained from the literatures [1,2]. The doping dependence of the carrier mobility and the minority carrier lifetime in the base region was also considered in the material library[3] and used for the simulation.

The npn epitaxial structure described at the Ref.[4] and the effects of variations in the doping and thickness of each layer were investigated to examine the influence to the transistor performance. In each case, the layer parameters were varied one at a time with all the others fixed and then the effects examined. The effects of the base doping were presented in Fig.1 in terms of f_{max} and f_T for the various base doping with a fixed base width of 450Å. The f_{max} and f_T increase with base doping and after reaching the peak they decrease again due to the impurity scattering. In addition, the high doping can induce the out-diffusion of impurity, resulting in reduction of current gain as shown in Fig.2a). Therefore, the optimum doping density of base was extracted from the product of the current gain and f_{max} as indicated in Fig.2b).

The collector doping is also known to influence the high frequency performance of the device since it effects the collector series resistance and delay time. As shown in Fig.3 the f_T and f_{max} were calculated for the various collector doping with a fixed collector width of 3000 Å. As the collector doping increased, f_T increased from 110GHz at $1x10^{16}/cm^3$ to 126GHz at $7x10^{16}/cm^3$ due to reduction in the base-collector space charge region width that results in a reduction in the collector delay time and a corresponding increase of f_T as shown in Fig.3. Simultaneously, f_{max} decreases as the collector capacitance increases with doping density. In Fig.4 the optimum collector doping density was extracted from the product of f_T*f_{max}.

Based on the above results, an optimized device structure was obtained as in Table I. The collector InP was inserted for the selective etching of InGaAs collector out of the sub-collector. The thickness of InP emitter is designed to be thick enough to prevent the electrical short between the emitter cap layer and the base when fabricated by self-align process.

3. Device fabrication

Based on the structure we fabricated the self-aligned HBTs. The selective wet etching of InP by HCl based solutions produces strong an-isotropic effects that depend on crystal orientation[5]. To make the edges of the masks parallel to the [010] and [001] crystal directions allowed the use of rectangular emitters while still avoiding the lack of undercut in the [01$\bar{1}$]. The first process step was the emitter formation by a wet of the emitter cap(InGaAs) and of the InP emitter. Fig.6 shows SEM images of device cross section whose edge is parallelly deployed to the [010] and [001] directions. The mesa produced the effect of the crystal orientation. The InP emitter serves as mask for the formation of a wet-etched undercut. The Ti/Au emitter- and base metal was deposited by evaporation and patterned by the lift-off technique. Subsequently, the base/collector mesa was formed by wet-etching and Ti/Au collector metal was deposited. In Fig.7 a Gummel plot of self-aligned InP/InGaAs HBT is measured by HP4155A and presented. The current gain was about 50 as similar as the design.

4. Conclusions

We have designed and fabricated InP/InGaAs HBTs. The current gain, f_{max} and f_T were obtained as the designed.

Acknowledgments

This work was supported by grant No.(R02-2000-00271) from the Basic Research Program of the Korea Science & Engineering Foundation.

References

[1] W. Liu, Handbook of Ⅲ-Ⅴ Heterojunction Bipolar Transistor, Wiley, P.1255, (1988)

[2] B. Jalali and S. J. Pearton, InP HBTs; Growth, Processing, and Applications, Atrech House, P.93, 1995

[3] S. Datta, et al., IEEE Trans. Electron Dev., vol.45, no.8, p.1634 1998

[4] H. Nakajima, et al.,Electron Lett., vol.29, no.21, p.1887, 1993

[5] N. Matine, et al., J.J.Appl.Phys. vol.38 p.1200, 1999

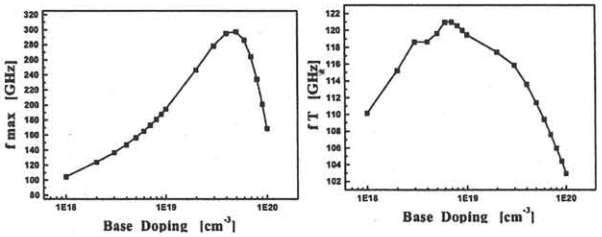

(a) (b)

Fig. 1 The calculated (a)f_{max} and (b) f_T as a function of the base doping.

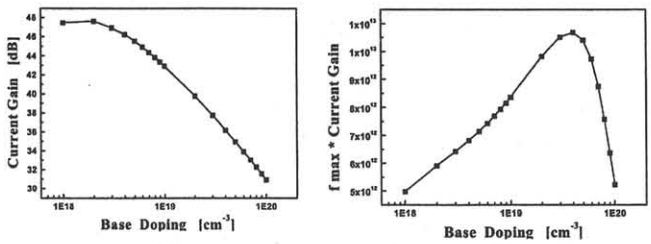

(a) (b)

Fig. 2 The calculated (a) current gain and (b) the current gain*f_{max} as a function of base doping.

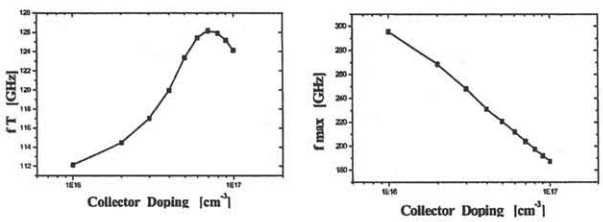

(a) (b)

Fig. 3 The calculated (a) f_T and (b) f_{max} as a function of collector doping

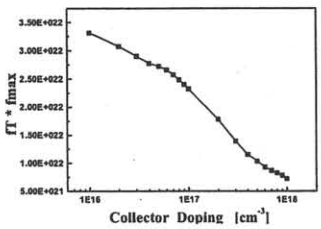

Fig. 4 The calculated f_T*f_{max} as a function of collector doping

Table I The epitaxial structure of InP/InGaAs HBT

Layer	Material	Thickness(Å)	Doping(cm^{-3})
Cap	N^+-InGaAs	1000	$3x10^{19}$
	N^+-InP	500	$2x10^{19}$
Emitter	N-InP	1500	$3x10^{17}$
Base	i-InGaAs	50	-
	p^+-InGaAs	450	$4x10^{19}$
Collector	n-InGaAs	3000	$1x10^{16}$
	N-InGaAs	500	$5x10^{18}$
	N-InP	300	$5x10^{18}$
Subcollector	n-InGaAs	4000	$5x10^{18}$

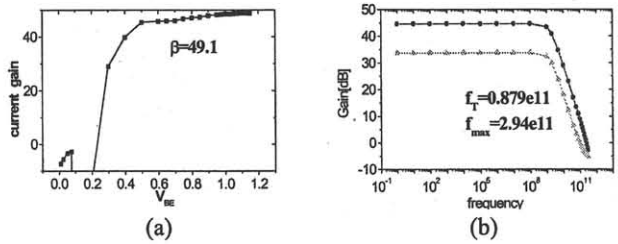

(a) (b)

Fig. 5 The alculated (a) current gain (b) f_T, f_{max} of the optimum device

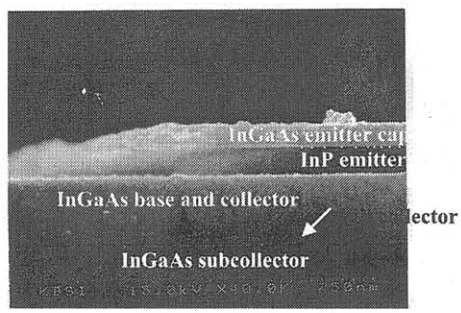

Fig. 6 The cross-sectional SEM view of InP/InGaAs HBT

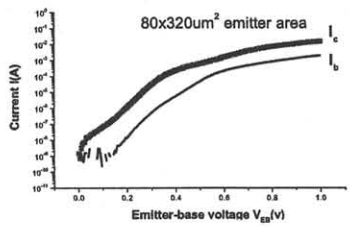

Fig. 7 The Gummel plot of the self-aligned 80×320um² HBT